Structural and Magnetic Properties of Fe50Al50 Nanocrystalline Alloys

by Kontan Tarigan

Journal of the Korean Physical Society, Vol. 57, No. 6, December 2010, pp. 1555∼1558

Structural and Magnetic Properties of $Fe_{50}Al_{50}$ Nanocrystalline Alloys

K. Tarigan, S. K. Oh, T. L. Phan and S. C. Yu*
BK-21 Physics Program and Department of Physics, Chungbuk National University, Cheongju 361-763, South Korea
D. S. Yang
Physics Division, School of Science Education, Chungbuk National University, Cheongju 361-763, South Korea

(Received 7 January 2010, in final form 26 June 2010)

The structural and the magnetic properties of nanocrystalline $Fe_{50}Al_{50}$ alloys prepared by using a mechanical alloying process (using commercial Fe and Al powders as precursors) were studied in detail as functions of the milling time for milling times ranging from 1 hr to 24 hrs. The structural analyses based on X-ray diffraction (XRD) and extended X-ray absorption fine structure spectroscopy (EXAFS) revealed that the alloying process took place after 12 hrs of milling. Using the Williamson-Hall plot, we found that the crystallite size decreased from to 220 to 14.3 nm while the strain increased from 5.32×10^{-3} to 19×10^{-3} when the milling time was varied from 1 hr to 24 hrs. Concerning the magnetic behavior, the data obtained from a superconducting quantum interference device (SQUID) showed that both the magnetic saturation (M_s) and the coercivity (H_c) depended strongly on the milling time and that these dependence were related to changes in the crystallite size. With these results, we believe that by adjusting the milling time, we can obtain an appropriate structural transformation and appropriate magnetization values.

PACS numbers: 75.75.-a, 75.50.Tx, 61.46.Df, 61.05.Cj, 61.05.C-
Keywords: $Fe_{50}Al_{50}$ nanoparticles, Structure and magnetic properties
DOI: 10.3938/jkps.57.1555

I. INTRODUCTION

Nanocrystalline materials obtained by high-energy ball milling are of great interest since it is known that those materials may exhibit different electrical, magnetic, optical, and other physical properties in the nano-regime due to finite size effects [1]. The formation of metastable phases and disorder in the crystal lattice through mechanical alloying (MA) gives interesting mechanical and magnetic properties. This is particularly evident in the case of the Fe-Al intermetallic system because the complicated phase diagrams and dependence of magnetic properties on disorder and microstructure make them interesting to study through the MA process. Furthermore, the Fe-Al systems are technologically important because of their superior mechanical properties and resistance to corrosion, besides their being amenable to easy substitution by other metal atoms. For these reasons, alloyed Fe-Al systems with various compositions have been investigated in recent years [2,3]. More particularly, the Fe-Al intermetallic compounds offer a combination of attractive properties, such as high specific strength, good strength at intermediate temperatures and excelent corrosion resistance at elevated temperatures under oxidizing, carburizing and sulfidizing atmosphere [4,5]. The degree of order in Fe-Al intermetallic alloys has an important influence on their magnetic properties. Moreover, the deformation of ordered alloys causes a dramatic increase in magnetization [6]. In Fe-Al alloys with the bcc structure, the magnetic moment of Fe atoms depends on the local structure. As a rule, Fe atoms with less than four nearest Fe neighbors possess no localized magnetic moments, and Fe atoms become magnetic only when they have four or more Fe nearest neighbors [7]. The magnetic properties of an assembly of small grains depend on the counter play between the local magnetic anisotropy energy and the ferromagnetic exchange energy [8].

In this work, we studied $Fe_{50}Al_{50}$ alloys by changing the milling time. Their structural and magnetic properties were then studied by means of X-ray diffraction (XRD), extended X-ray absorption fine structure spectroscopy (EXAFS), and superconducting quantum interference device (SQUID).

*E-mail: scyu@chungbuk.ac.kr; Tel: +82-43-261-2269; Fax: +82-43-274-7811

II. EXPRIMENTAL DETAILS

$Fe_{50}Al_{50}$ nanocrystalline alloys were prepared by mechanical alloying using a SPEX 8000 mixer with stainless-steel balls and a stainless-steel vial. The starting mixture of $Fe_{50}Al_{50}$ was formed by using commercial powders of Fe (53 μm, 99.9%) and Al (53-106 μm, 99.9%). For the milling, the weight ratio of the ball-to-powder was 5:1. $Fe_{50}Al_{50}$ alloys were mixed and ground for differing times of 1, 2, 4, 6, 12, and 24 hrs. This process was performed in an Ar ambien[18] avoid oxidation.

After the preparation, magnetic measurements were carried out by using a superconducting quantum interference device (SQUID). The sizes of the particles and their morphologies were checked preliminarily by using scanning electron microscopy (SEM). XRD data were obtained by using an X-ray diffractometer with the Cu-K_α radiation. Based on these data, the crystallite size and the strain of the samples w[28] estimated in terms of the Williamson-Hall method. Extended X-ray absorption fine structure (EXAFS) data were collected from the 3C1 EXAFS beam line of the Po[23]g Light Source (PLS). The PLS was operated at an energy of 2.5 GeV and a maximum current of 200 mA. EXAFS spectra were obtained at the Fe K-edge (7112 eV) in the transmission mode at room temperature. After that, the EXAFS data were analyzed by making use of the IFEFFIT software. The structural properties are discussed in connection with the magnetic properties of the alloys.

III. [22]RESULTS AND DISCUSSION

Figure 1 shows typical SEM images revealing the variations in particle shape and size of the $Fe_{50}Al_{50}$ powders after 2, 12, and 24 hrs of milling. Our SEM study revealed that the particles present in the $Fe_{50}Al_{50}$ samples had quite similar shapes, where very small particles were located on the surfaces of big particles. The [30]ticle size varied as we changed the milling time. The average particle sizes estimated from the SE[13] images decreased with increasing milling time. Such results are in good agreement with the data estimated by using the Williamson-Hall plot.

XRD patterns obtained from the $Fe_{50}Al_{50}$ nanocrystalline alloys are shown in Fig. 2. All the peaks after 12 hrs of milling are broader and shifted to smaller angles, which are due to the deformation of the structure and variation in the crystallite size. The deformation is due to the replacement Fe atoms by Al atoms, which signals the format[27] of an alloy. Based on these XRD data, the crystallite size and the lattice strain can be evaluated from the intercept and slope of the Williamson-Hall plot [9]:

$$B\cos\theta = (K\lambda/D) + 2\epsilon\sin\theta, \quad (1)$$

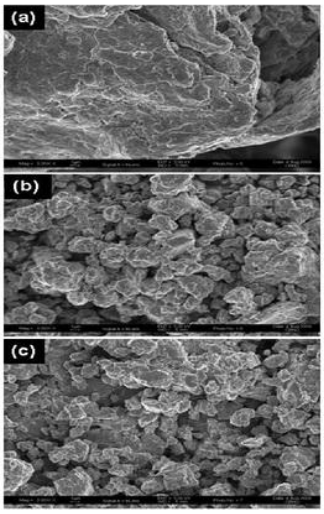

Fig. 1. Typical SEM ima[24] for $Fe_{50}Al_{50}$ nanocrystalline alloys with milling times of (a) 2 hrs, (b) 12 hrs, and (c) 24 hrs.

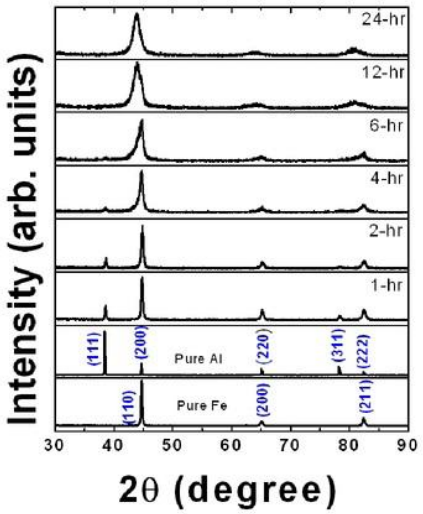

Fig. 2. XRD patterns of $Fe_{50}Al_{50}$ with different milling times.

where B is the FWHM in radians, D is the average [17]rystallite size, ϵ is the strain, K is the shape factor, λ is the X-ray wavelength and *theta* is the Bragg angle.

Figure 3 shows the [25]rystallite size and the strain of the samples as functions of the milling time. The crystallite size and the strain of the sample after a 1-hr of milling were found to be about 220 nm and 5.32×10^{-3}, respectively. After a 24-hr of milling, the crystallite size decreased to ∼13.5 nm while the strain increased to 19.03

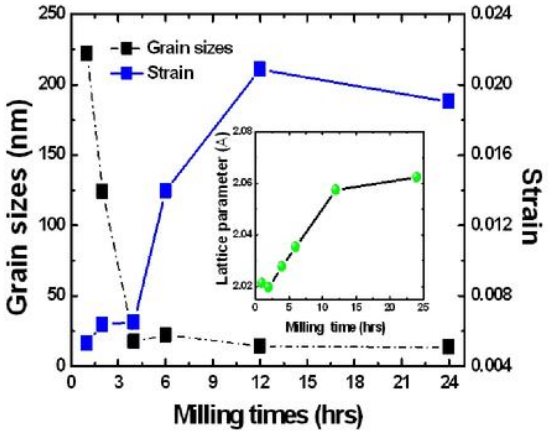

Fig. 3. Crystallite size (dashed-dotted line) and strain (solid line) for $Fe_{50}Al_{50}$ nanocrystalline alloys as functions of the milling time. The inset shows the variation of the lattice parameter based on (110) peak with respect to the milling time.

$\times 10^{-3}$. The inset of Fig. 3 presents the variation of the lattice parameter, calculated from Scherrer's formula (here, the 110 peak of the $Fe_{50}Al_{50}$ was fitted to a Gaussian function); it increases slightly from 2.01 to 2.06 Å.

Figure 4(a) shows the Fourier transform of the EXAFS spectra of the $Fe_{50}Al_{50}$ alloys measured at the Fe K-edge for various milling times. The radial atomic density in real space can be seen in the Fourier-transformed spectra [10]. The dotted lines shown in Fig. 4(a) indicate the first, second, third, and fourth shells of pure Fe, which are guidelines to compare with alloyed samples. The magnitude of the Fourier-transformed spectrum decreased when the milling time was increased. This suggest that the number of Fe-Fe bonds are decreased due to the inter-diffusion of Fe and Al atoms. In addition, the first and the fourth shells were shifted, corresponding to the increased Fe-Al bonding. This indicates that the short- and the long-range orders increased with increasing milling time. Clearly, the 12- and the 24-hr milled samples exhibit different positions of the phase in the first and the fourth shells compared to the 1-, 2-, 4-, and 6-hr milled samples. This can be explained by a change in the Fe-Fe order due to alloy formation of Fe-Al. Such results are in good agreement with the XRD data. These changes in the local structural order caused the variation in the magnetic properties of the samples. Here, EXAFS was used to examine the local structure of the samples. Variations in amplitude and the shift of an EXAFS peak give information on the structural changes occurring in the MA process on an atomic scale. The reduction of the amplitude in the EXAFS spectrum can be caused by spatial and chemical disorders. Most spatial disorder causes variations in the phases in EXAFS spectra. Figure 4(b) shows the k-weighted EXAFS spectra

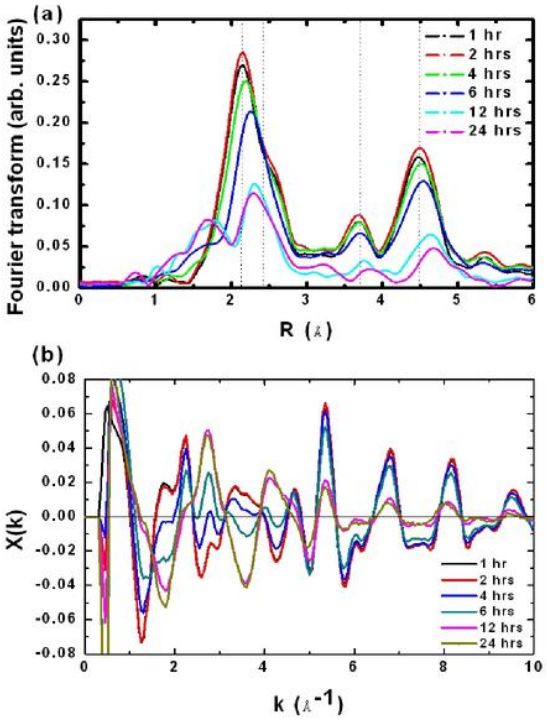

Fig. 4. (Color online) (a) Fourier transform measured at the Fe K-edge and (b) k-weighted EXAFS spectra for mechanically-alloyed $Fe_{50}Al_{50}$ for different milling times.

of $Fe_{50}Al_{50}$ powders processed for 1, 2, 4, 6, 12, and 24 hrs. The decrease in the amplitude before a 12-hr milling indicates that the fracture and the cold welding of both Fe and Al were dominant and that a minor change in the local structure had occurred. However, a significant change in the phase took place for the sample with a milling time of 12 hrs. This indicates that the alloying process was dominant, and that a new phase was formed for this sample. The amount of the new phase increased as the milling time was increased. Such a situation influences the magnetic properties of the samples strongly, as will be presented below.

In Fig. 5, the magnetization and the coercivity are shown as functions of the milling time. One can see that magnetization rapidly decreases in the initial stage of the milling (lower milling time) because changes in the structure of mixed powder from Fe grains to $Fe_{50}Al_{50}$ grains occur [10,11]. Beginning at a 2-hr milling and after, the magnetization decreased slowly. This variation of the magnetization could come from the dilution of the magnetic lattice of Fe caused by Al with increasing milling time. In Fig. 5, one can also see that the coercivity (H_c) increases with increasing the milling time, reaching a maximum value at about 225 Oe after a 6-hr milling,

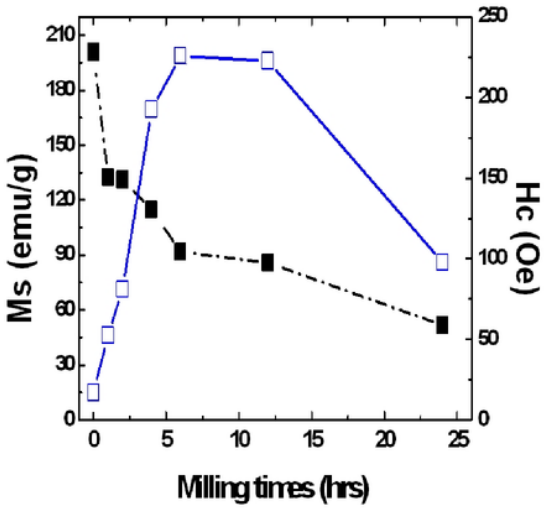

Fig. 5. Magnetic saturation (dashed-dotted line) and coercivity (solid line) for $Fe_{50}Al_{50}$ alloys as functions of the milling time.

and it decreases to about 100 Oe after a 24-hr milling. The H_c increase for a relatively short milling time can be attributed to a reduction in the crystallite size. Meanwhile, the decreases in H_c for a longer milling time indicate an increased formation of the Fe-Al alloy. Further milling tended to make all samples highly disordered, then, they lost part of their high magnetic anisotropy, and the H_c was reduced [12]. Furthermore, one can see from Figs. 3 and 5 that magnetic saturation decreased as the lattice parameter increased.

IV. CONCLUSION

The formations of $Fe_{50}Al_{50}$ metastable alloys were explicitly shown in the XRD patterns with shifted and broadened peaks. EXAFS spectra showed variations in the amplitude and the phase for the samples with milling times of 12 and 24 hrs. The significant change in the phase confirmed that new Al atoms were introduced around the central Fe atoms during the MA process. The magnetization saturation was decreased due to magnetic dilution caused by the Al. Meanwhile, the coercivity decreased due to growing single-domain size and reduced particle size.

ACKNOWLEDGMENTS

This research was supported by the Basic Science Research Program through the National Research Fondation of Korea (NRF) found by the Ministry of Education Science and Technology (2010-0013155).

REFERENCES

[1] P. Kameli, H. Salamati and A. Aezami, J. Appl. Phys. **100**, 053914 (2006).
[2] V. Sebastian, N. Lakshmi and K. Venugopalan, J. Intermetalic **15**, 1006 (2007).
[3] A. Hernando, X. Amils, J. Nogues, S. Surinach, M. D. Baro and M. R. Ibarra, Phys. Rev. B **58**, R11864 (1998).
[4] H. Shi, D. Guo and Y. Ouyang, J. Alloys Compd. **455**, 2008).
[5] D. P. Dutta, G. Sharma, A. K. Rajarajan, S. M. Yusuf and G. K. Dey, J. Chem. Mater. **19**, 6 (2007).
[6] D. M. Rodriguez, E. Apinaniz, F. Plazaola, J. S. Garitaonandia, J. A. Jimenez, D. S. Schmool and G. J. Cuello, ys. Rev. B **71**, 212408 (2005).
[7] L. F. Kiss, J. Balogh, D. Kaptás, T. Kemény and I. Vincze, Rev. Adv. Mater. Sci. **18**, 505 (2008).
[8] G. erzer, IEEE Trans. Magn. **26**, 5 (1990).
[9] S. Dutta, S. Chattopadhyay, M. Sutradhar, A. Sarkar, M. Chakrabarti, D. Sanyal and D. Jana, J. Phys. Condens. Matter **19**, 236218 (2007).
[10] H. Shokrollahi, J. Mater. Des. **30**, 3374 (2009).
[11] H. Nam, J. Korean Ceram. Soc. **39**, 11 (2002).
[12] J. Sort, S. Surinach, J. S. Munoz and M. D. Baro, Phys. Rev. B **65**, 174420 (2002).

Structural and Magnetic Properties of Fe50Al50 Nanocrystalline Alloys

ORIGINALITY REPORT

18%	10%	17%	%
SIMILARITY INDEX	INTERNET SOURCES	PUBLICATIONS	STUDENT PAPERS

PRIMARY SOURCES

1	www.e-arm.org Internet Source	1%
2	M. M. Rajath Hegde. "Phase transformation, structural evolution, and mechanical property of nanostructured feal as a result of mechanical alloying", Powder Metallurgy and Metal Ceramics, 04/21/2010 Publication	1%
3	S. Vives, E. Gaffet, C. Meunier. "X-ray diffraction line profile analysis of iron ball milled powders", Materials Science and Engineering: A, 2004 Publication	1%
4	Jiraskova, Y., J. Bursik, O. Zivotsky, and J. Cuda. "Influence of Fe2O3 on alloying and magnetic properties of Fe–Al", Materials Science and Engineering B, 2014. Publication	1%
5	www.cheric.org Internet Source	

1%

6 Moritz Trautvetter. "Thermally driven solid-phase epitaxy of laser-ablated amorphous AlFe films on (0001)-oriented sapphire single crystals", Applied Physics A, 08/04/2010 — 1%
Publication

7 Jartych, E.. "Magnetic properties and structure of nanocrystalline Fe-Al and Fe-Ni alloys", Nanostructured Materials, 1999 — 1%
Publication

8 Manikam, Vemal Raja, Khairunisak Abdul Razak, and Kuan Yew Cheong. "A novel silver–aluminium high-temperature die attach nanopaste system: the effects of organic additives content on post-sintered attributes", Journal of Materials Science Materials in Electronics, 2013. — 1%
Publication

9 Chandrasekhar, R.. "The effects of samarium addition on CoCrTa-based thin films for magnetic recording", Journal of Magnetism and Magnetic Materials, 19960302 — 1%
Publication

10 Haddad, Ahmed, and Mohammed Azzaz. "Eddy Current Characterization of $(Fe_{65}Co_{35})_xAl_{1-x}$ Nanocrystalline Alloy Synthesized by — 1%

Mechanical Alloying Process", Key Engineering Materials, 2013.
Publication

---

11 Ullah, Zaka, Shahid Atiq, and Shahzad Naseem. "Influence of Pb doping on structural, electrical and magnetic properties of Sr-hexaferrites", Journal of Alloys and Compounds, 2013. 1%
Publication

---

12 J. Balogh. "Magnetic properties of superparamagnet/ferromagnet heterostructures", physica status solidi (c), 12/2004 1%
Publication

---

13 S. Brotzmann. "Diffusion and defect reactions between donors, C, and vacancies in Ge. I. Experimental results", Physical Review B, 06/2008 1%
Publication

---

14 D. S. Yang. "Improved R-space resolution of EXAFS spectra using combined regularization methods and nonlinear least-squares fitting", Physical Review B, 08/1996 1%
Publication

---

15 ieeexplore.ieee.org 1%
Internet Source

---

npl.csircentral.net

16	Internet Source	1%
17	Botcharova, E.. "Supersaturated solid solution of niobium in copper by mechanical alloying", Journal of Alloys and Compounds, 20030310 Publication	1%
18	www.victoria.ac.nz Internet Source	1%
19	worldwidescience.org Internet Source	1%
20	binaryoptionstradinglist.com Internet Source	1%
21	Fathi, M.H.. "Fabrication and characterization of fluoridated hydroxyapatite nanopowders via mechanical alloying", Journal of Alloys and Compounds, 20090505 Publication	<1%
22	nsti.org Internet Source	<1%
23	Hyun Joon Shin. "Optical design of the U7 undulator beamline at the Pohang Light Source", Journal of Synchrotron Radiation, 5/1/1998 Publication	<1%
24	P. Kamatchi Subramanian. "Selective Laser	

	Sintering of Alumina Using Aluminum Binder", Materials and Manufacturing Processes, 07/01/1995 Publication	<1%
25	Aguilar, C.. "A thermodynamic approach to energy storage on mechanical alloying of the Cu-Cr system", Scripta Materialia, 200708 Publication	<1%
26	Dimple P. Dutta, Garima Sharma, A. K. Rajarajan, S. M. Yusuf, G. K. Dey. "Study of Magnetic FeAl Nanoparticles Synthesized Using a Chemical Route", Chemistry of Materials, 2007 Publication	<1%
27	Schmitt, M.-T., J. E. Hoffmann, and D. Eifler. "Thermal stability of nanocrystalline electrodeposited nickel-iron : Thermal stability of nanocrystalline electrodeposited nickel-iron", physica status solidi (a), 2013. Publication	<1%
28	www.qucosa.de Internet Source	<1%
29	Fan, R.H.. "The bonding character and magnetic properties of Fe"3Al: Comparison between disordered and ordered alloy", Physics Letters A, 20061225 Publication	<1%

30 Dutta, H.. "Microstructure characterization of polymorphic transformed ball-milled anatase TiO"2 by Rietveld method", Materials Chemistry & Physics, 20030102
Publication

<1%

Exclude quotes	Off	Exclude matches	Off
Exclude bibliography	Off		